# Prompt-Based Segmentation at Multiple Resolutions and Lighting Conditions using Segment Anything Model 2

Osher Rafaeli<sup>®</sup>, Tal Svoray<sup>®</sup>, Roni Blushtein-Livnon<sup>®</sup> and Ariel Nahlieli

Abstract—This paper provides insight into the effectiveness of zero-shot, prompt-based, Segment Anything Model (SAM), and its updated version, SAM 2, and the non-promptable, conventional convolutional network (CNN), in segmenting solar panels, in RGB aerial imagery, across lighting conditions, spatial resolutions, and prompt strategies. SAM 2 demonstrates improvements over SAM, particularly in sub-optimal lighting conditions when prompted by points. Both SAMs, prompted by user-box, outperformed CNN, in all scenarios. Additionally, YOLOv9 prompting outperformed user points prompting. In high-resolution imagery, both in optimal and sub-optimal lighting conditions, Eff-UNet outperformed both SAM models prompted by YOLOv9 boxes, positioning Eff-UNet as the appropriate model for automatic segmentation in high-resolution data. In lowresolution data, user box prompts were found crucial to achieve a reasonable performance. This paper provides details on strengths and limitations of each model and outlines robustness of user prompted image segmentation models in inconsistent resolution and lighting conditions of remotely sensed data.

Index Terms—SAM 2, YOLO, EfficientNet, Solar panels, Transfer learning.

### I. INTRODUCTION

Remote sensing involves gathering information about the terrestrial Earth's surface, water bodies and the atmosphere via airborne or satellite platforms, serving a wide range of applications [1]. Recent advances in computer vision (CV) facilitated automatic pixel-level classification analyses and improved greatly image segmentation [2].

The end-to-end network, denoted Convolutional Neural Network (CNN), was found successful in image segmentation tasks. CNN-based models typically obtain semantic representations using stacked convolutions and pooling operations restoring image size by upsampling [3]. Based on the well-know U-shaped network, various improved encoder—decoder designs were applied [4]. For example, the noval architecture Eff-UNet combines the effectiveness of compound scaled pretrained EfficientNet as the encoder for feature extraction with UNet decoder for reconstructing fine-grained segmentation maps [5].

CNN-based image segmentation depends on training quality in terms of diversity, and representativeness and the model's ability to address similar tasks after training [6]. Recently, Prompt-based Vision Transformer (ViT) models which enable users interactively to control outputs during prediction, became

more commonly-used [7]. These models allow correcting errors along the process and visualizing ongoing predictions [8].

Prompt-based models can enhance prediction from zero-Shot (where a model classifies classes it hasn't encountered during training), allowing generalization based on learning underlying concepts/relationships of the data and interpret and respond to new, unseen, input data [9]. Meta FAIR gained progress with zero-Shot prompt-based image segmentation during 2023-24. Segment anything model (SAM) demonstrates this by conducting image segmentation with minimal human intervention. It only requires a bounding box or a clicked point for a prompt [10]. Furthermore, when SAM is guided by YOLO-generated box prompts [11], entire segmentation pipeline can become end-to-end automatically [12]. Since SAM release, at 2023, the scientific community has expressed large interest to implement it for remote sensing purposes, integrating SAM in various applications [13]. Particularly, throughout 2024, engineers invested many resources to develop adapters for improving SAM accuracy to handle remotely sensed data [14].

SAM 2 was introduced in late July 2024, extending promptable visual segmentation. According to Meta research, based on enormous datasets, SAM 2 outperforms the previous version in terms of accuracy and inference time. SAMs are trained and tested on ground-level photographs and videos [15], thus, they still encounter challenges when applied to remote sensing imagery. For instance, low-resolution images, imbalance between background and targets, inconsistency in lighting and atmospheric conditions, may lead to differences in appearance of various objects of interest, and can limit the effectiveness of segmentation models [16].

Our *aim* here, is to compare three segmentation approaches: (1) The conventional fully automatic CNNs, including trained conventional Eff-UNet with pre-trained on ImageNet EfficientNet encoder and classic U-Net; (2) CV-promptable SAM and SAM 2, prompted with bounding boxes generated by YOLOv9 object detection model; and (3) semi-automatic approach implementing user-promptable SAMs prompted by user created bounding boxes and one-click centroid points. Within this comparison we outline two objectives: (1) to investigate effects of the following prompt strategies on model performance in SAM and SAM 2: user-created points, usercreated bounding boxes, and CV-generated bounding boxes using YOLO; and (2) to estimate models' performance using three airborne datasets with low-resolution (0.25 m) and highresolution (0.15 m) under optimal and sub-optimal lighting conditions.

O. Rafaeli, R. Blushtein-Livnon and A. Nahlieli are with the Department of Environmental, Geoinformatics and Urban Planning Sciences, Ben-Gurion University of the Negev, Israel (e-mail: osherr@post.bgu.ac.il; livnon@bgu.ac.il; arielnah@post.bgu.ac.il).

T. Svoray is with the Department of Environmental, Geoinformatics and Urban Planning Sciences, and the Department of Psychology, Ben-Gurion University of the Negev, Israel (e-mail: tsvoray@bgu.ac.il).

# II. MATERIALS AND METHODOLOGY

The study setup was designed to conduct the comparison between the three segmentation approaches described in the research aims in the end of the Introduction section and as can be seen in Fig. 1.

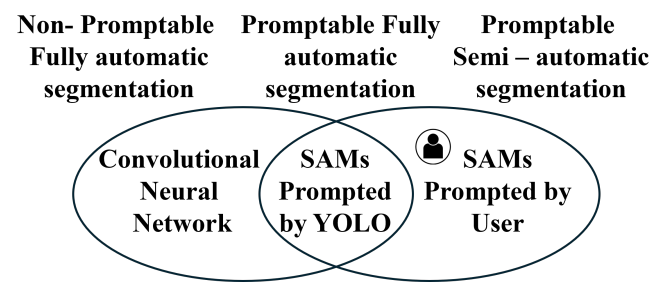


Fig. 1. The three approached compared in study setup,

# A. Study area

A rural area near Be'er Sheva, Israel, was selected because it is characterized by scattered settlements, agricultural fields, and large rangelands, posing a challenge for the models' effectiveness in identifying small-scale photovoltaic (PV) cells, in sparsed-target environments, with varying land-uses. Airborne images of the studied area were obtained spanning three years with varying resolutions and lighting conditions: 2022 for high resolution (0.15 m) with optimal lighting conditions, 2017 for high resolution (0.15 m) with sub-optimal lighting conditions, and 2015 for low resolution (0.25 m). These datasets were used to assess models' performance across image qualities. Overall 3000 PV cells were identified and labeled in each airborne dataset as illustrated in Fig. 2.



Fig. 2. PV cells captured in images with different resolutions and lighting conditions: High resolution (0.15 m) and low-resolution image (0.25 m), highlighting the increased difficulty in segmentation as resolution decreases and lighting condition becomes sub-optimal.

# B. Data preparation

Following the airborne survey, aerial photo interpretation and annotation were conducted to generate precise masks of PV cells. These masks serve as the basis for: (1) training the CNN models, Eff-UNet, U-Net and the YOLO; (2) generating user prompts in a semi-automatic approach, which includes bounding boxes and centroid points, as illustrated in Fig. 3; and (3) estimate models performance on unseen data.



Fig. 3. User Prompts: bounding boxes and centroid points

# C. Eff-UNet

Convolutional neural network progressively reduces the input image resolution to obtain the high level feature map representing the original image and the decoder module consists of a set of layers that upsamples the feature map of encoder to recover spatial information. We implemented here encoder path with the cutting edge set of CNN EfficientNet, introduced in 2019 by Google AI research [17]. For decoder, U-Net allows the network to propagate context information to higher-resolution layers. In our implementation, we used EfficientNetB1 pretrained on ImageNet utilizing transfer learning to adapt it for our specific PV cells segmentation task. Additionally, we implemented a simple U-Net to generate baselines to models.

# D. YOLO

You Only Look Once (YOLO) proposes end-to-end neural network object localization and detection models. The speed and accuracy of YOLO models made them widespread in scientific and industrial applications [18]. Here, YOLO models provided bounding-box generation for PV cells in the aerial images. These automatic bounding boxes were then used to prompt both SAM and SAM 2. During the intermediate tests, We trained and evaluated the three latest state-of-the-art YOLO models: YOLOv8 [19], YOLOv9 [20], and YOLOv10 [21] to identify the most suitable model for our PV cells segmentation. YOLOv9 was chosen by us as it outperformed YOLOv8 and YOLOv10 in detecting the small PV cells in challenging scenarios (Table I).

TABLE I Comparison of YOLO versions

	YOLOv8	YOLOv9	YOLOv10
IoU	0.602	0.630	0.611
F1-score	0.692	0.724	0.703

# E. Training and Implementation Details

PV cell images and corresponding ground truth masks were processed into patches of 256 x 256 pixels and randomly divided into training, validation, and test sets, with 70% (2100 PV cells) of the labels used to train the Eff-UNet, YOLOv9 and U-Net models, 10% (300 PV cells) for validation, and

20% (600 PV cells) for testing. The models were trained with 75 epochs, a batch size of 4 images, and an initial learning rate of 0.001. The learning rate decayed exponentially. Dice Loss Function was employed for UNet and Eff-UNet:

Dice Loss = 
$$1 - \frac{2 \times |A \cap B|}{|A| + |B|}$$
 (1)

where A and B are the predicted and ground truth binary segmentations, respectively. The intersection  $|A \cap B|$  represents the common elements, while |A| and |B| denote the total number of elements in each segmentation.

Our implementation utilized high-performance computational resources to ensure efficient training and inference of the segmentation models. Specifically, we employed the Ultralytics YOLOv8.2.71 framework [22] with PyTorch-2.3.1 for YOLO and SAMs, and Keras module from TensorFlow library for U-Net and EfficientNet. All was running on Python 3.9.15 with an NVIDIA RTX A4000 GPU.

### F. Segment anything models

The above prompts were used as an input to SAM and to SAM 2. We used both models in their large configurations to maximize accuracy. All prompting points are used as input together as foreground prompts to the SAM models, while for bounding boxes masks were extracted for each bounding box separately, and then, all image prediction were combined. If more than a single object occurred in a single image, we combined prediction by choosing pixels with higher foreground probability. The same procedure was used with bounding boxes detected by YOLOv9.

# G. Model performance metrics

To assess models performance, we employed the widely recognized evaluation metrics in equation 2:

Accuracy = 
$$\frac{TP + TN}{TP + FN + TN + FP}$$

$$Precision = \frac{TP}{TP + FP}$$

$$Recall = \frac{TP}{TP + FN}$$

$$F1 Score = 2 \times \frac{Precision \times Recall}{Precision + Recall}$$

$$IoU = \frac{|A \cap B|}{|A \cup B|}$$
(2)

where TP, TN, FP, and FN denote, respectively, the true positive, true negative, false positive, and false negative values, and A and B represent the predicted and ground truth segments, respectively. IoU denotes Intersection over Union.

# III. RESULTS

Performance of segmentation models was analyzed for high-resolution images, with optimal and sub-optimal lighting conditions, and low-resolution images. The different models include: Segment Anything Models with user points and user box, YOLOv9 generated Boxes, CNN non-promotable models, Eff-UNet and U-Net baseline model.

# A. High-Resolution with optimal lighting conditions

The user box prompts for both SAM and SAM 2 with an IoU of 0.79 and F1-score of 0.88, outperformed the other model configurations. A slight decline in performance was observed in point prompted SAMs that achieved an IoU of 0.65 and F1-score of 0.77. Among the fully automatic models, Eff-UNet outperformed with an IoU of 0.71 and F1-Score of 0.79. Similar to SAM and SAM 2, prompted by YOLOv9, that achieved an IoU of 0.68 and F1-Score of 0.77, see Fig. 4.

# B. High-Resolution with sub-optimal lighting conditions

Under sub-optimal lighting conditions, we identified significant variability in performance across segmentation models, see Fig. 4. SAM models prompted by user box performed consistently better than other models. SAM 2 prompted by user boxes slightly outperforms with an IoU of 0.77 and F1-Score of 0.86, while SAM achieved an IoU of 0.75 and F1-Score of 0.85. However, when prompted by points, SAM 2 markedly surpasses SAM, with an IoU of 0.57 and an F1-Score of 0.69, while SAM dropped significantly achieving an IoU of 0.51 and F1-Score of 0.63. SAM prompted by points results in partially segmented PV cells and falsely part of the background as PV cells. This decreases both Recall and Precision. By contrast, SAM 2 does not demonstrate this bias and thus performs better. Among the automatic models, Eff-UNet achieved an IoU of 0.64 and an F1-Score of 0.73. Similarly, the performance of SAMs models prompted by YOLOv9 generated boxes aligned closely with IoU of 0.63 and F1-Score of 0.72.

### C. Low-Resolution

Both SAM models with manually generated box prompts demonstrate reasonable accuracy even under low-resolution conditions, achieving an IoU of 0.69 and F1-score of 0.81. By contrast to user box prompts, the SAM models with usergenerated points struggle to extract correctly the boundaries of PV cells, achieving a low IoU of 0.36 and F1-Score to 0.42. The performance of all automatic models, also declined under the low-resolution conditions. Even Eff-UNet, which had achieved the best results at higher resolutions struggled to effectively learn patterns and extract these features from unseen tested data, as well as YOLOv9 that also struggled to supply reliable boxes as prompts to SAM models, see Fig. 4.

# D. Mean Performance Across Resolutions and conditions

When averaging the accuracy measures across resolutions and conditions (Table II), SAM 2 model with user box prompts showed consistently high performance across resolutions, indicating its robustness in various conditions. Achieving an IoU of 0.75 and an F1-Score of 0.85. Similarly SAM 2 outperforms SAM with points prompt that achieved an IoU of 0.51 and F1-Score of 0.62. SAMs prompted by YOLOv9 outperformed user single click prompts. Eff-UNet and SAMs promoted by YOLOv9 showed similar performance with an IoU of 0.55 and F1-Score of 0.64, see Fig. 5.

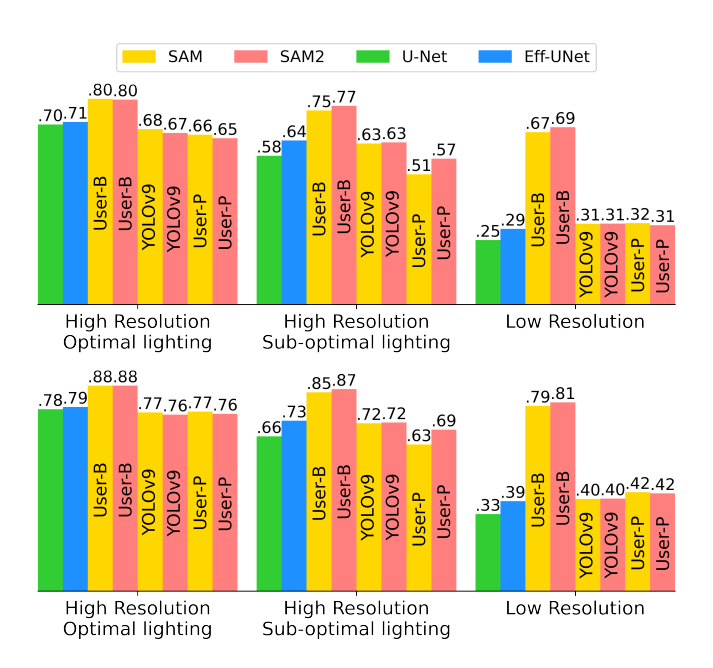


Fig. 4. IoU (upper chart) and F1-score (lower chart) results across unseen datasets

TABLE II Metrics for models across different unseen datasets

	User- Points		User-Box		Box (YOLOv9)		Eff-UNet (U-Net)
	SAM	SAM2	SAM	SAM2	SAM	SAM2	
IoU	0.49	0.51	0.74	0.75	0.54	0.54	0.55 (0.51)
F1	0.61	0.62	0.84	0.85	0.63	0.63	0.64 (0.59)
Prec.	0.54	0.53	0.82	0.81	0.63	0.61	0.68 (0.62)
Rec.	0.88	0.92	0.89	0.92	0.66	0.68	0.64 (0.61)
Acc.	0.97	0.98	1.00	1.00	1.00	1.00	1.00 (1.00)

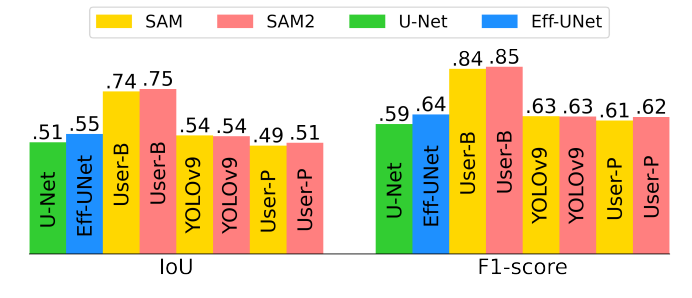


Fig. 5. Mean IoU and F1 score results across all unseen datasets

# IV. CONCLUSION

Assessment of models performance includes accuracy estimation and a consideration of the resources invested in the segmentation process. In most scenarios, annotation by humans yielded the highest accuracy but it is labor intensive. The following insights into these trade-offs, focusing on new prompt-based segmentation methods, that use expert prompts to reduce usage of precise manual annotation, are drawn:

(1) Based on Iou and F1-Score, SAM 2 outperforms SAM, particularly under sub-optimal lighting conditions. Primarily, SAM 2 segments PV cells in full while SAM segments it only partially or segments falsely part of the background as PV cell, see Fig. 6. Additionally, when PV panels are clustered,

SAM tends to segment black objects near the panels as PV cells, while SAM 2 handles this scenario more precisely, segmenting only the PV cells accurately, see Fig. 7. SAM 2's improvements in remote sensing imagery segmentation may be attributed to its new architecture and its training on a diverse dataset that includes challenging small objects [15].

- (2) YOLO boxes as a prompt input to SAM and SAM 2 computations outperforms even single click by human annotators. Predicted boxes lead to even lower false positive rate (FPR) by better defining foreground and background regions. This occurs particularly in scenes with sub-optimal light conditions and shadowing effect, see Fig. 8.
- (3) Under fully automatic segmentation approach, in high-resolution imagery, Eff-UNet and SAM prompted by YOLO performance, are similar, while Eff-UNet slightly outperforms. This may occur by SAM prompt-ability attribute, which expects user prompts. When fed by an imperfect CV object detection model, such as YOLO, SAM places high weight on these prompts, thus false positive boxes fed into SAM. This can lead to erroneously segmented objects, potentially involving many pixels. Consequently, SAM segments almost completely YOLO truly detected panels while Eff-UNet may segment it partially, see Fig. 9. Conversely, when the model is not fed by a true positive object, it does not segment any pixels of this object. By contrast, Eff-UNet does not exhibit this bias and thus perform more consistently.

Finally, when using high-resolution datasets with well-defined objects, the use of trained CNN models is preferable. Their use allows a single training process on well-defined data and subsequent prediction. Conversely, given varying resolution, and mainly light conditions, of many time series of remotely sensed data, where fully automatic models struggle, human prompts in SAM models, offer significant advantages. Even under low-resolution conditions, SAM prompted by user prompts achieved a reasonable accuracy. Further research is recommended to thoroughly test our findings on other less-defined objects and/or satellites and drone data.

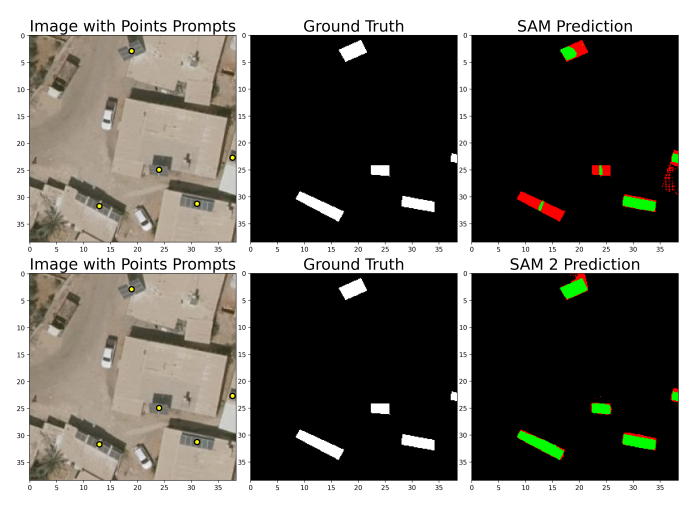


Fig. 6. SAM Vs. SAM 2: Under sub-optimal lighting imagery, SAM 2 segments PV cells in full while SAM segments them partially, or falsely, SAM segments background pixels as PV cells (Green - TP, Red - FP and FN predicted PV pixels).

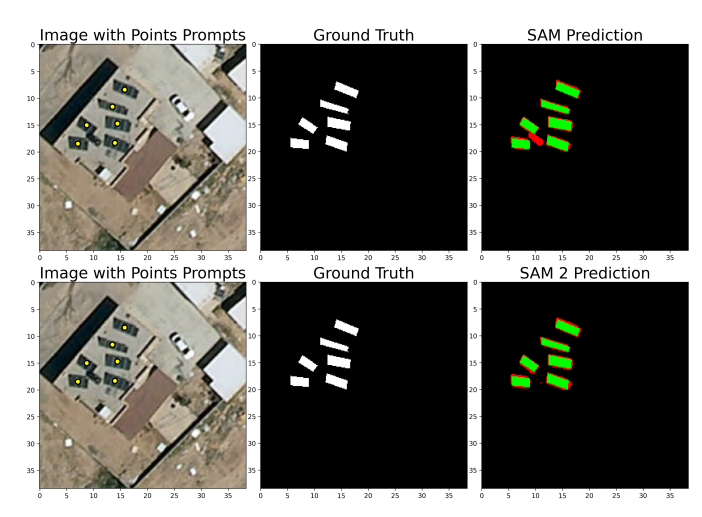


Fig. 7. SAM Vs. SAM 2: Clustered black objects are segmented by SAM as PV cells (Red-FP and FN) whereas SAM 2 accurately segments only the PV cells (Green-TP).

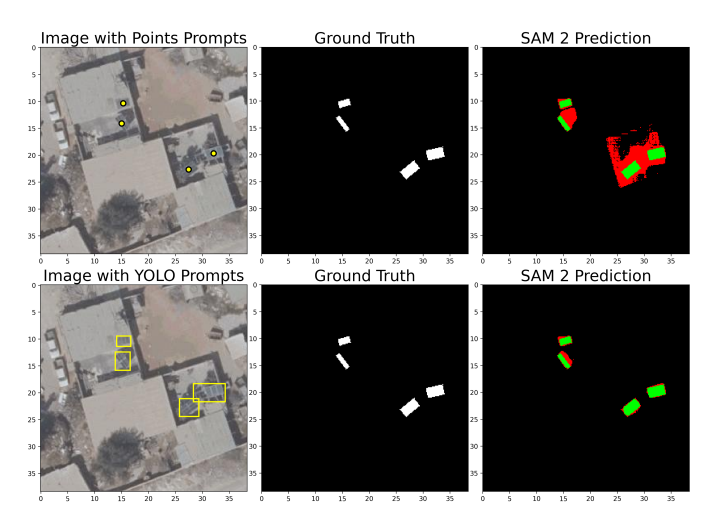


Fig. 8. Prompts performance: YOLO exceeds single click prompts. boxes lead to lower FP rate by defining the foreground and background regions. (Green-TP, Red-FP and FN predicted PV pixels).

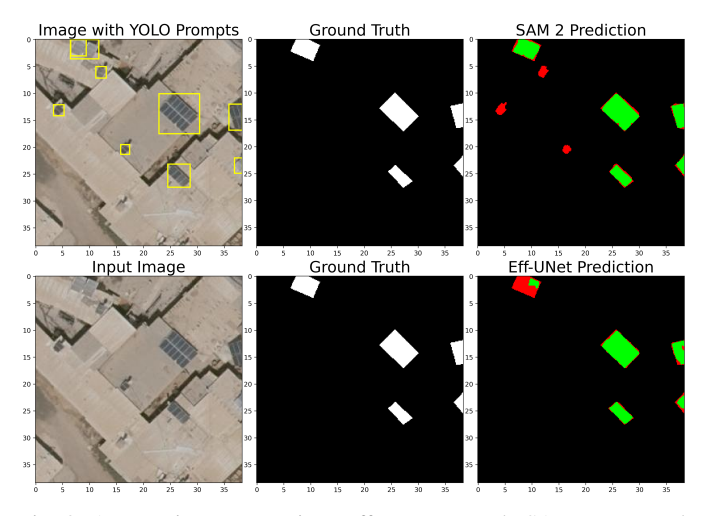


Fig. 9. Automatic segmentation: Eff-UNet exceeds SAMs prompted by YOLO. SAM heavily weights these prompts, causing false positives to affect many pixels (Green - TP, Red - FP and FN).

### ACKNOWLEDGMENT

We thank Israel Science Foundation (ISF), grant 299/23, Ministry of Agriculture Chief Scientist, grant 16-17-0005, 2022, and Negev Scholarship by the Kreitman School of Ben-Gurion University that support Osher Rafaeli's PhD studies.

### REFERENCES

- [1] F. Sabins and J. Ellis, *Remote Sensing: Principles, Interpretation, and Applications*. Waveland Press, Incorporated, 2020.
- [2] L. Ma, Y. Liu, X. Zhang, Y. Ye, G. Yin, and B. A. Johnson, "Deep learning in remote sensing applications: A meta-analysis and review," *ISPRS Journal of Photogrammetry and Remote Sensing*, vol. 152, pp. 166–177, 2019.
- [3] O. Ronneberger, P. Fischer, and T. Brox, "U-net: Convolutional networks for biomedical image segmentation," *CoRR*, vol. abs/1505.04597, 2015.
- [4] X. X. Zhu, D. Tuia, L. Mou, G.-S. Xia, L. Zhang, F. Xu, and F. Fraundorfer, "Deep learning in remote sensing: A comprehensive review and list of resources," *IEEE Geoscience and Remote Sensing Magazine*, vol. 5, no. 4, pp. 8–36, 2017.
- [5] B. Baheti, S. Innani, S. Gajre, and S. Talbar, "Eff-unet: A novel architecture for semantic segmentation in unstructured environment," in 2020 IEEE/CVF Conference on Computer Vision and Pattern Recognition Workshops (CVPRW), pp. 1473–1481, 2020.
- [6] P. Sharma, Y. P. S. Berwal, and W. Ghai, "Performance analysis of deep learning cnn models for disease detection in plants using image segmentation," *Information Processing in Agriculture*, vol. 7, no. 4, pp. 566–574, 2020.
- [7] T. Lüddecke and A. Ecker, "Image segmentation using text and image prompts," in *Proceedings of the IEEE/CVF Conference on Computer Vision and Pattern Recognition (CVPR)*, pp. 7086–7096, June 2022.
- [8] M. A. Mazurowski, H. Dong, H. Gu, J. Yang, N. Konz, and Y. Zhang, "Segment anything model for medical image analysis: An experimental study," *Medical Image Analysis*, vol. 89, p. 102918, 2023.
- [9] S. Pratt, I. Covert, R. Liu, and A. Farhadi, "What does a platypus look like? generating customized prompts for zero-shot image classification," 2023
- [10] A. Kirillov, E. Mintun, N. Ravi, H. Mao, C. Rolland, L. Gustafson, T. Xiao, S. Whitehead, A. C. Berg, W.-Y. Lo, P. Dollár, and R. Girshick, "Segment anything," 2023.
- [11] J. Redmon, S. Divvala, R. Girshick, and A. Farhadi, "You only look once: Unified, real-time object detection," in 2016 IEEE Conference on Computer Vision and Pattern Recognition (CVPR), pp. 779–788, 2016.
- [12] Y. Zhu, Q. Yang, and L. Xu, "Active learning enabled low-cost cell image segmentation using bounding box annotation," 2024.
- [13] L. P. Osco, Q. Wu, E. L. de Lemos, W. N. Gonçalves, A. P. M. Ramos, J. Li, and J. M. Junior, "The segment anything model (sam) for remote sensing applications: From zero to one shot," 2023.
- [14] D. Wang, J. Zhang, B. Du, M. Xu, L. Liu, D. Tao, and L. Zhang, "Samrs: Scaling-up remote sensing segmentation dataset with segment anything model," in *Advances in Neural Information Processing Systems* (A. Oh, T. Naumann, A. Globerson, K. Saenko, M. Hardt, and S. Levine, eds.), vol. 36, pp. 8815–8827, Curran Associates, Inc., 2023.
- [15] N. Ravi, V. Gabeur, Y.-T. Hu, R. Hu, C. Ryali, T. Ma, H. Khedr, R. Rädle, C. Rolland, L. Gustafson, et al., "Sam 2: Segment anything in images and videos," arXiv preprint arXiv:2408.00714, 2024.
- [16] A. Moghimi, M. Welzel, T. Celik, and T. Schlurmann, "A comparative performance analysis of popular deep learning models and segment anything model (sam) for river water segmentation in close-range remote sensing imagery," *IEEE Access*, vol. 12, pp. 52067–52085, 2024.
- [17] M. Tan and Q. V. Le, "Efficientnet: Rethinking model scaling for convolutional neural networks," CoRR, vol. abs/1905.11946, 2019.
- [18] T. Diwan, G. Anirudh, and J. V. Tembhurne, "Object detection using yolo: Challenges, architectural successors, datasets and applications," multimedia Tools and Applications, vol. 82, no. 6, pp. 9243–9275, 2023.
- [19] D. Reis, J. Kupec, J. Hong, and A. Daoudi, "Real-time flying object detection with yolov8," arXiv preprint arXiv:2305.09972, 2023.
- [20] C.-Y. Wang, I.-H. Yeh, and H.-Y. M. Liao, "Yolov9: Learning what you want to learn using programmable gradient information," arXiv preprint arXiv:2402.13616, 2024.
- [21] A. Wang, H. Chen, L. Liu, K. Chen, Z. Lin, J. Han, and G. Ding, "Yolov10: Real-time end-to-end object detection," arXiv preprint arXiv:2405.14458, 2024.
- [22] G. Jocher, A. Chaurasia, and J. Qiu, "Ultralytics yolo," jan 2023. Available: https://github.com/ultralytics/ultralytics.